Journal of Materials Science: Materials in Electronics
https://doi.org/10.1007/s10854-019-02212-0

Microwave dielectric properties of $BaO–ZnO–B_2O_3–P_2O_5$ glass–ceramic for LTCC application

B. B. Lu[1] · J. Huang[1] · D. H. Jiang[1] · J. J. Chen[1] · J. Xu[1] · J. Xi[1] · G. H. Chen[1] · F. Shang[1] · J. W. Xu[1] · C. L. Yuan[1] · C. R. Zhou[1]

Received: 5 August 2019 / Accepted: 16 September 2019

Abstract
A new $10BaO–40ZnO–15B_2O_3–35P_2O_5$ (wt%) glass–ceramic with ultra-low permittivity and excellent thermal stability were fabricated by solid-state reaction method. The sintering, phase composition, microstructure and microwave dielectric properties of the glass–ceramics were studied through XRD, SEM, density and dielectric property measurement. The result shows $BaZn_2(PO_4)_2$ precipitates first at low sintering temperature of 550 °C, and with increasing sintering temperature, $Zn_3(PO_4)_2$ and $Zn_3(BO_3)_2$ phases come out in succession in the glass. The bulk densities of the glass–ceramics firstly increase and then decrease with the increment of firing temperature and the highest density can be achieved at 700 °C. The glass–ceramics sintered at 700 °C for 2.5 h possesses the optimal dielectric properties of $\varepsilon_r = 4.16$, $Q \times f = 12{,}250$ GHz (13.6 GHz), and $\tau_f = -1.5$ ppm/°C. Moreover, the samples have good chemical compatibility with silver electrodes, which indicates that the developed glass–ceramic materials are suitable for LTCC applications.

1 Introduction

LTCC technology is an important technology in microelectronic field. It requires that materials could be co-fired with metals such as copper and silver at lower temperatures [1, 2]. With the integration and multifunction of passive implements, it is particularly important to find a LTCC substrate materials with low dielectric constant (ε_r) and low loss [3, 4]. In general, the low dielectric constant has a direct influence on the signal transmission speed, the frequency selective characteristics of the device are determined by the quality factor ($Q \times f$) of the materials, the thermal stability of the device lies on the temperature coefficient of the resonant frequency (τ_f) [5, 6]. Therefore, microwave dielectric ceramics with low ε_r, high $Q \times f$ and a near zero τ_f are expected to solve the above problems.

Conventional microwave ceramics such as $BaTi_4O_9$, $Ba_2Ti_9O_{20}$ and $LiAl_{1-x}(Mg_{0.5}Si_{0.5})xO_2$ have excellent microwave dielectric properties, but the sintering temperature exceeds 1300 °C, which is impossible to co-fire with electrodes such as Ag or Al [7–9]. At present, LTCC material systems with low ε_r have been reported, such as molybdates, vanadates and tungstates [10–12]. These systems have inherent low sintering temperature and good dielectric properties, but they have poor chemical compatibility with metal electrodes such as copper and silver during co-firing process [13, 14]. Bian et al. [15, 16] reported these compounds including $A_2P_2O_7$ (A = divalent metal), $CaCuP_2O_7$, $SrCuP_2O_7$, $CaZnP_2O_7$ and $SrZnP_2O_7$, and found these compounds sintered at 900 °C have good dielectric properties: $\varepsilon_r = 7$, $Q \times f = 10{,}000$ GHz and $\tau_f = -70$ ppm/°C. However, the large τ_f and ε_r limit its application. Song et al. [17] reported that 1 wt% LiF added $0.7BaAl_2Si_2O_8–0.3Ba_5Si_8O_{21}$ ceramic sintered at 750 °C has excellent microwave dielectric properties of $\varepsilon_r = 7.63$, $Q \times f = 12{,}410$ GHz and $\tau_f = -1.2$ ppm/°C. However, the ε_r is somewhat high.

Recently, divalent metallic phosphate and borate compounds have relatively low ε_r and high Q value [18, 19]. Došler et al. [20] reported that $MgO–B_2O_3–SiO_2$ glass–ceramic sintered at 850–950 °C showed the dielectric properties of $\varepsilon_r = 6.1–6.9$, $Q \times f = 5000–8000$ GHz (12 GHz). Qing et al. [21] found that adding ZnO to $CaO–Al_2O_3–SiO_2$ can reduce the permittivity and increase the $Q \times f$ value. Jiang et al. [22] reported that $CaO–ZnO–B_2O_3–P_2O_5$ glass–ceramics exhibited good dielectric properties of $\varepsilon_r = 4.2–6.5$, $Q \times f = 13{,}450–16{,}826$ GHz (13.44 GHz),

✉ G. H. Chen
cgh1682002@163.com

[1] School of Material Science and Engineering, Guangxi Key Laboratory of Information Materials, Guilin University of Electronic Technology, Guilin 541004, China

Published online: 19 September 2019

$\tau_f = -21$ to -25 ppm/°C when sintered at 650–780 °C. As we know, Ba^{2+} has a large ion radius and inhibits the migration of alkali metal ions, it can effectively reduce dielectric loss of glass–ceramic. Simultaneously, BaO, as a typical network modifier oxide in glass, will destroy the original network structure to some extent. Therefore, the addition of BaO in the glass composition will decrease softening temperature and enhance the liquidity of the glass phase, and promote densification within a certain range. Zhu et al. [23] found that adding BaO to $CaO–B_2O_3–SiO_2$ could reduce glass transition temperature and softening temperature. Hence, if BaO substitutes for CaO in $CaO–ZnO–B_2O_3–P_2O_5$, it is expected that a new glass–ceramic substrate material with preeminent microwave dielectric properties and with low sintering temperature can be obtained.

In this work, $BaO–ZnO–B_2O_3–P_2O_5$ glass–ceramics were prepared by solid state reaction route, and its microstructure, phase composition, microwave dielectric properties and co-firing compatibility with Ag were carefully studied.

2 Experimental procedure

The preparation process of glass–ceramics is divided into two parts, including the preparation of glass and glass–ceramics. For synthesizing glass powders, the chemical raw materials $BaCO_3$ (≥ 99.0%), ZnO (≥ 99.0%), H_3BO_3 (≥ 99.5%) and $NH_4H_2PO_4$ (≥ 99.0%) (Shanghai Guoyao Co., Ltd., China) were weighed and blended according to designed glass composition of $10BaO–40ZnO–15B_2O_3–35P_2O_5$ (abbreviated to BZBP, wt%). The mixed batch was melted in a high purity aluminum crucible in air at 1300 °C for 2 h. The glass melt was quenched, and milled to fine powder. For preparing glass–ceramics, the 12% polyvinyl alcohol was added into BZBP glass powder as binder and pressed into cylinder (12 mm diameter, 5–6 mm height) under a uniaxial pressure of 4 MPa. In order to eliminate the binder, all the pellets were heated to 500 °C for 1 h, and then maintained at scheduled sintering temperatures for 150 min in air to make glass–ceramics.

The absorption spectrum of the sample is obtained in the range of 400–4000 cm^{-1} through Fourier transform infrared spectrum for revealing the structure of glass. The glass transition temperature and crystallization temperature of BZBP glasses were investigated by differential thermal analysis (DTA) using alumina as the reference material, at a heating rate of 10 °C/min. The phase composition of the samples was analyzed by XRD. The bulk density (ρ) of the sintered pellets was measured by the Archimedes method. Microwave dielectric properties of the samples were measured by network vector analyzer, and the test frequency is between 13 and 14 GHz. The microstructure of the sample and its chemical compatibility with Ag electrodes were observed by SEM equipped with EDS. The temperature coefficient of resonate frequency (τ_f) in a temperature range of 25–75 °C was calculated using the formula [24] $\tau_f = (f_T - f_0)/f_0(T - T_0)$, where f_T and f_0 are the resonate frequencies at the measuring temperature T and room temperature T_0 (25 °C), respectively.

3 Results and discussion

Figure 1 displays the FTIR spectra of the BZBP glass. Six absorption peaks are observed. The absorption peaks of the glass structure are illustrated in two infrared regions. The first one appears near 708 cm^{-1}, which owes to the bending vibration of the B–O–B bond [25]. The asymmetric stretching vibration of B–O bond in BO_3 triangle, corresponding to the other peak appears near 1440 cm^{-1}. The peak at 484 cm^{-1} indicates the formation of Zn–O bond [25]. The tensile vibration of the P=O bond is corresponding to the peak at 1100 cm^{-1}. The presence of absorption peaks of 2350 cm^{-1} and 3430 cm^{-1} indicates the presence of water groups (OH), which is caused by the moisture absorption during the preparation of the samples using KBr [25].

Figure 2 shows DTA curve and XRD pattern of BZBP glass. The glass transition temperature (T_g) is 524 °C, two exothermic peaks, which corresponds to 603 °C and 659 °C, represent different crystallization temperature. XRD pattern shows that the precursor glass exhibits a broad dispersion peak, which indicates that BZBP glass is not crystallized, i.e. a typical amorphous substance.

Figure 3 shows XRD profiles of BZBP glass samples sintered at different temperatures. XRD analysis results demonstrate that the glass starts to precipitate the $BaZn_2(PO_4)_2$ phase when sintered at 550 °C. As the sintering temperature increases to 600 °C, the new phase $Zn_3(PO_4)_2$ appears. With further increasing firing temperature from 660 to 740 °C,

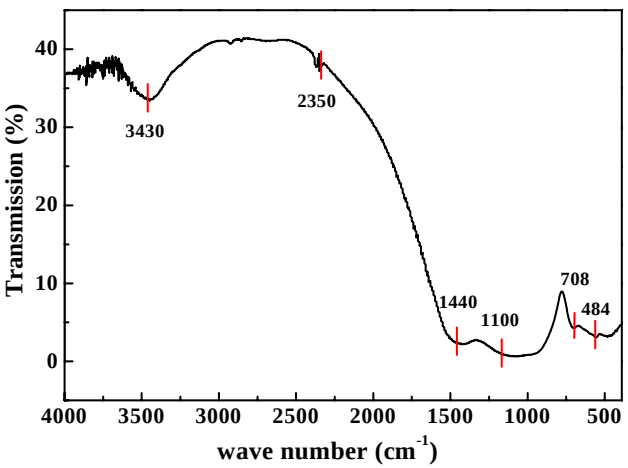

Fig. 1 FTIR spectra of glass

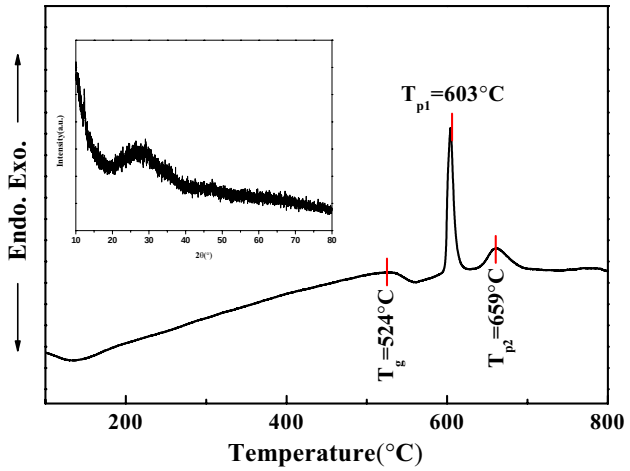

Fig. 2 DTA curve and XRD pattern of glass

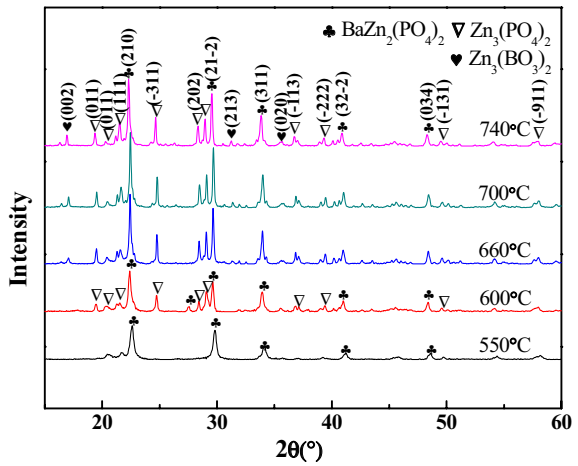

Fig. 3 XRD profiles of the glass specimens sintered at various temperatures

three types of phases including $BaZn_2(PO_4)_2$, $Zn_3(PO_4)_2$, and $Zn_3(BO_3)_2$ coexist. According to XRD patterns, it can be clearly seen that $BaZn_2(PO_4)_2$ phase is the main phase. Based on the change of diffraction intensity, the crystal phase content of the sample gradually increases with the increase of temperature. When the sintering temperature reaches 740 °C, the diffraction intensity obviously decreases because of over-sintering of the sample. Table 1 shows the phase composition of the samples at different sintering temperatures.

Figure 4 illustrates the bulk densities of glass–ceramics. The specimen sintered at 550 °C is not densified and has a minimum density. With the increment of temperature from 550 to 740 °C, the density firstly increases remarkably and then decreases. And a maximum value of 3.26 g/cm^3 can be gained at 700 °C, which is due to the dense microstructure of

Table 1 Phase composition of the specimens obtained at various temperatures

Sintering temperature (°C)	Phase compositions		
550	$BaZn_2(PO_4)_2$		
600	$BaZn_2(PO_4)_2$	$Zn_3(PO_4)_2$	
660	$BaZn_2(PO_4)_2$	$Zn_3(PO_4)_2$	$Zn_3(BO_3)_2$
700	$BaZn_2(PO_4)_2$	$Zn_3(PO_4)_2$	$Zn_3(BO_3)_2$
740	$BaZn_2(PO_4)_2$	$Zn_3(PO_4)_2$	$Zn_3(BO_3)_2$

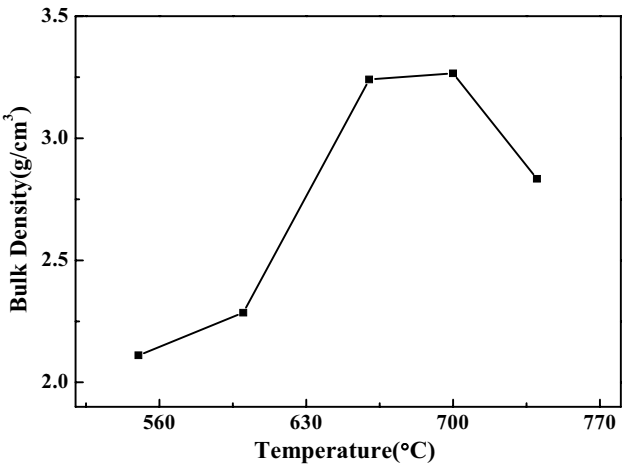

Fig. 4 Bulk density of the specimens at various temperatures

the sample. Nevertheless, the decrease in density at 740 °C is the result of excessive sintering [19]. Hence, bulk density is directly affected by sintering temperature [26].

SEM micrographs of the samples at different sintering temperatures are shown in Fig. 5. It can be seen from Fig. 5 that at different sintering temperatures, the densification situation of the microstructure in the samples is obviously different. The samples sintered at 550 °C and 600 °C exhibit porous microstructure and contain a large amount of glass phase, indicating that the density of the sample is low. Obvious crystal phase precipitation and grain growth accompanied by less porosity are observed with raising sintering temperature from 660 and 700 °C. At present, liquid phase wets glass powder and promote the migration and rearrangement of particles, meanwhile, the crystal is further precipitated from the glass matrix. This is beneficial to sintering densification of the samples. The uniform and well-densified glass–ceramic can be obtained at 700 °C. However, with increasing sintering temperature up to 740 °C, excessive growth of some crystals is observed, which suppresses the sintering densification, namely, too high temperature will go against the sintering. The above results agree with the change of density of the samples, as shown in Fig. 4.

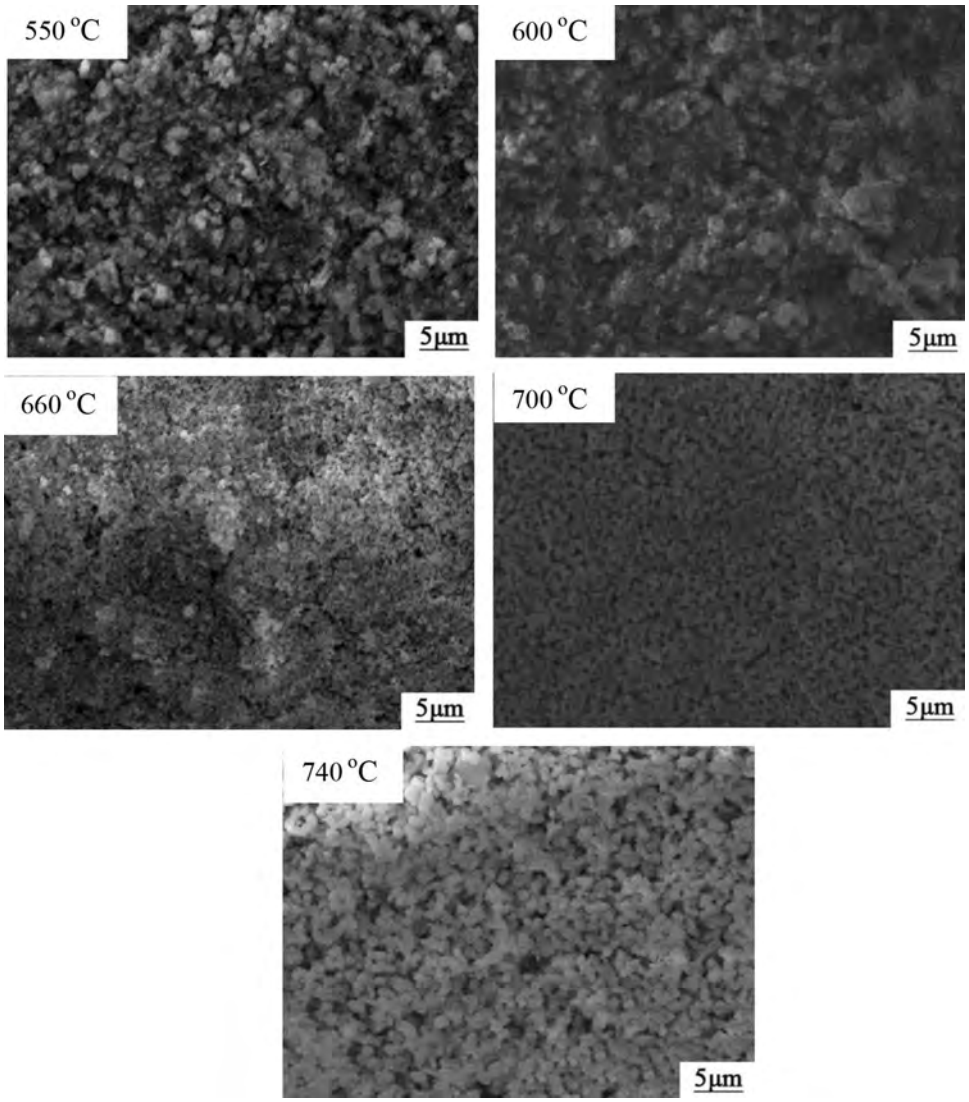

Fig. 5 SEM images of the samples sintered at various firing temperatures

Figure 6 demonstrates the permittivity of the glass–ceramic specimens at various sintering temperatures. With an increase in sintering temperature, the dielectric constant exhibits firstly raise and then reduce, which is in accord with variation tend of bulk density shown in Fig. 4. At 550 °C, the sample has the lowest permittivity due to porous microstructure and more glass phase with lower permittivity. At 600 °C and 660 °C, the permittivity increases obviously, which may be due to the relatively large dielectric constant and relatively compact microstructure of the main crystalline phase $BaZn_2(PO_4)_2$. When the sintering temperature continues to rise to 700 °C, the maximum dielectric constant is obtained, which is mainly ascribed to uniform and dense microstructure of the sample. However, when the sintering temperature reaches 740 °C, the dielectric constant decreases significantly, which is due to the increase of porosity. As well known, in glass ceramic materials, the dielectric constant of the

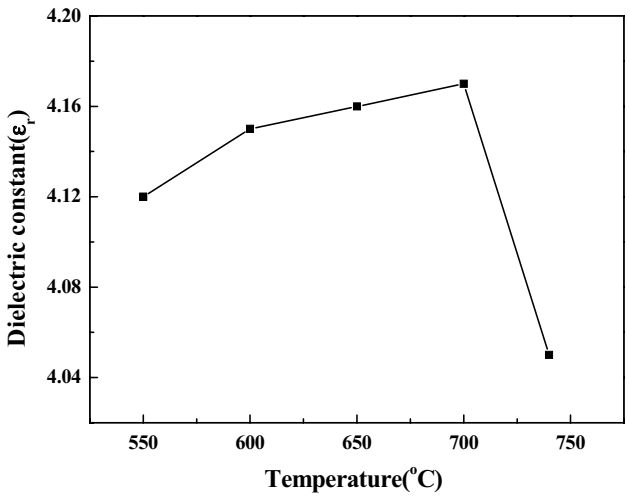

Fig. 6 Permittivity of the samples at various temperatures

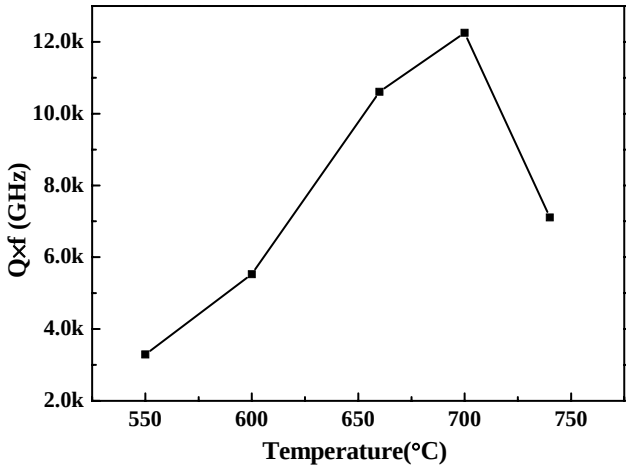

Fig. 7 Q×*f* values of the samples as a function of sintering temperatures

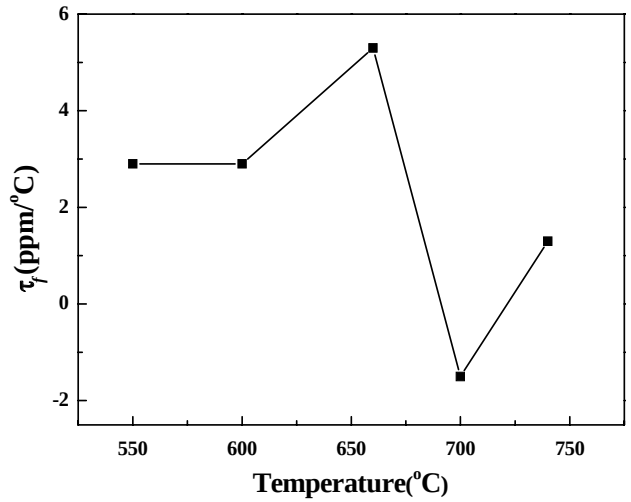

Fig. 8 The τ_f values of the glass–ceramics as a function of temperature

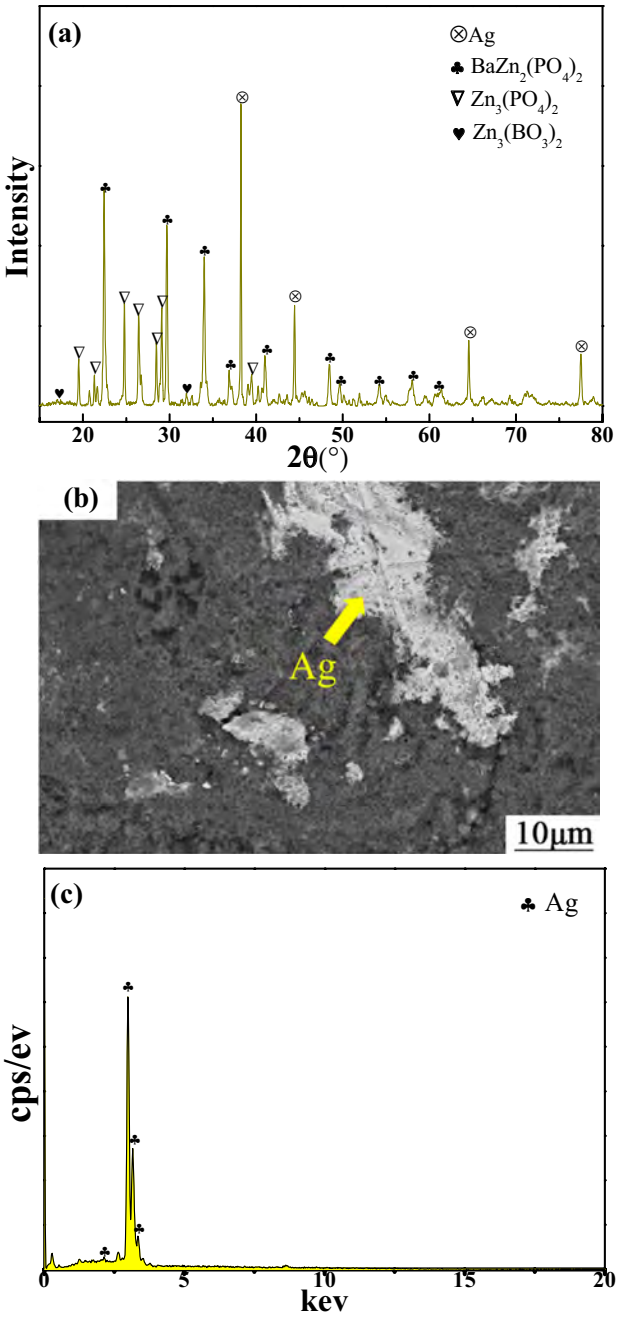

Fig. 9 **a** XRD pattern, **b** SEM image and **c** EDS analysis result of the specimen co-fired with 20 wt% silver at 700 °C for 150 min

sample is determined by the contents of crystalline phase, glass phase and pores.

Figure 7 displays Q × f values of the sintered glass–ceramic specimens. Generally, the quality factor (or dielectric loss) lies on not only by the intrinsic loss such as the lattice vibration modes, but also by type and content of crystal phase and densification of the sample [27, 28]. The influence of sintering temperature on the Q × f value of glass ceramics is similar to the trend of bulk density changing with sintering temperature, as seen in Fig. 4. In other words, with the increment of temperature, Q × f values display first augment and then diminish. When the sintering temperature is 700 °C, the Q × f value of the sample reaches a maximum of 12,250 GHz. For polycrystalline glass ceramics, the residual glass phase, the type of crystalline phase and the degree of densification all affect the Q × f value. It can be estimated that the Q × f values of $BaZn_2(PO_4)_2$, $Zn_3(PO_4)_2$ and $Zn_3(BO_3)_2$ exceed 15,000 GHz, respectively [6, 29]. With the increase of sintering temperature, the sample gradually becomes dense and the degree of crystallinity also increases. It is clear that the Q × f value of glass ceramics elevating with

Table 2 Sintering temperature and dielectric properties of some glass–ceramic systems

Glass–ceramic system	Sintering temperature (°C)	ε_r	Q×*f* (GHz)	τ_f (ppm/°C)
$CaO–B_2O_3–SiO_2$ [19]	800–950	5.5–6.5	1500–5000	− 51
$MgO–B_2O_3–SiO_2$ [20]	850–950	6.1–6.9	5000–8000	–
$CuO–B_2O_3–Li_2O$ [31]	625	5.84	10,120	− 33
$CaO–B_2O_3–SiO_2+La_2O_3$ [32]	825	4.1	8800	–
$BaO–ZnO–B_2O_3–P_2O_5$ [this work]	550–740	4.02–4.18	3300–12,250	− 1.5 to 5.3

the increase of the total crystalline phase. At 550 °C, the glass ceramics have the minimum Q × f value, which is due to the low sintering temperature, resulting in a large number of glass phases with low Q × f value and low density in the system. With further enhancing temperature from 600 to 700 °C, the decrease in the content of glass phase and pore results in obvious increase of Q × f values monotonously because the precipitated crystal phases have a higher Q × f value than that of glass phase. Assuredly, the Q × f value has been a great improvement because of dense microstructure. At 740 °C, the crystalline phase composition is almost parallel, and the Q × f value shows a significant decrease, which could be attributed to the increase of porosity in the sample caused by excessive sintering.

Figure 8 exhibits the τ_f values of BZBP glass–ceramics at different temperatures. It is found that the τ_f values vary slightly from − 1.5 to 3.5 ppm/°C. Obviously, the τ_f value is not sensitive to sintering temperature. In a word, all the glass–ceramics have good thermal stability.

To evaluate chemical compatibility of silver electrode with the glass–ceramic substrate, 20 wt% Ag powders were mixed with precursor glass powders and sintered at 700 °C for 150 min [30]. Figure 9 illustrates the XRD, SEM and EDS results of co-fired sample. It is found that only $BaZn_2(PO_4)_2$, $Zn_3(PO_4)_2$, $Zn_3(BO_3)_2$ and Ag can be observed, indicating the absence of any reaction nearly between glass–ceramic and silver. From the SEM micrographs, white region is on behalf of silver, whereas the dark regions are depicted as glass–ceramic material. Hence, the obtained glass–ceramics meet the demand for LTCC application.

Comparing with some glass–ceramic materials with low permittivity, as displayed in Table 2, the as-prepared glass–ceramic has reasonable processing temperatures and good microwave dielectric properties.

4 Conclusions

The $10BaO–40ZnO–15B_2O_3–35P_2O_5$ (wt%) glass–ceramics were fabricated by traditional solid phase method. The change of sintering temperature has a considerable influence on the phase composition, micro-structural morphology and microwave dielectric performance. The optimal dielectric properties of $\varepsilon_r = 4.16$, Q × *f* = 12,250 GHz (13.61 GHz) and $\tau_f = -1.5$ ppm/°C could be obtained at 700 °C for 150 min. The as-manufactured glass–ceramic, which possesses good chemical compatibility and microwave dielectric properties, is suitable for LTCC applications.

Acknowledgements This work was financially supported by National Undergraduate Innovation Program of the Ministry of Education of China (Grant Nos. 201810595014, 201810595015).

References

1. H. Zhou, J. Huang, X. Tan, N. Wang, G. Fan, X. Chen, Compatibility with silver electrode and microwave dielectric properties of low firing $CaWO_4$-$2Li_2WO_4$ ceramics. Mater. Res. Bull. **89**, 150–153 (2017)
2. C.C. Xia, D.H. Jiang, G.H. Chen, Y. Luo, B. Li, C.L. Yuan, C.R. Zhou, Microwave dielectric ceramic of $LiZnPO_4$ for LTCC applications. J. Mater. Sci.: Mater. Electron. **28**, 12026–12031 (2017)
3. M.T. Sebastian, H. Jantunen, Low loss dielectric materials for LTCC applications: a review. Int. Mater. Rev. **53**, 57–90 (2008)
4. S.Y. Chang, H.F. Pai, C.F. Tseng, C.K. Tsai, Microwave dielectric properties of ultra-low temperature fired Li_3BO_3 ceramics. J. Alloys Compd. **698**, 814–818 (2017)
5. S.N. Renjini, S. Thomas, M.T. Sebastian, Microwave dielectric properties and low temperature sintering of $Sm_2Si_2O_7$ ceramic for substrate applications. Int. J. Appl. Ceram. Technol. **6**, 286–294 (2009)
6. H. Yu, K. Ju, K. Wang, A novel glass-ceramic with ultra-low sintering temperature for LTCC application. J. Am. Ceram. Soc. **97**, 704–707 (2014)
7. Y. Choi, J.H. Park, W.J. Ko, S. Nahm, J.G. Park, Low temperature sintering of $BaTi_4O_9$-based middle-k dielectric composition for LTCC applications. J. Electroceram. **14**, 157–162 (2005)
8. M.R. Varma, H. Sreemoolanadhan, V. Chandrasekaran, Effect of different raw materials on the microwave dielectric properties of $Ba_2Ti_9O_{20}$ ceramics. J. Mater. Sci.: Mater. Electron. **15**, 345–349 (2004)
9. X.K. Lan, J.P. Li, J. Li, Z.Y. Zou, G.F. Fan, W.Z. Lu, W. Lei, Lattice structure and microwave dielectric properties of $[Mg0.5Si0.5]^{3+}$-doped $LiAlO_2$ solid solution. J. Mater. Sci.: Mater. Electron. **30**, 11764–11770 (2019)
10. M.T. Sebastian, H. Wang, H. Jantunen, Low temperature co-fired ceramics with ultra-low sintering temperature: a review. Curr. Opin. Solid State Mater. **20**, 151–170 (2016)
11. D. Zhou, C.A. Randall, H. Wang, Microwave dielectric ceramics in Li_2O-Bi_2O_3-MoO_3 system with ultra-low sintering temperatures. J. Am. Ceram. Soc. **93**, 1096–1100 (2010)

12. H. Zhou, Y. Miao, J. Chen, Sintering characteristic, crystal structure and microwave dielectric properties of a novel thermally stable ultra-low firing $Na_2BiMg_2V_3O_{12}$ ceramic. J. Mater. Sci.: Mater. Electron. **25**, 2470–2474 (2014)
13. M. Valant, D. Suvorov, Chemical compatibility between silver electrodes and low-firing binary-oxide compounds: conceptual study. J. Am. Ceram. Soc. **83**, 2721–2729 (2000)
14. H.T. Yu, J.S. Liu, W.L. Zhang, S.R. Zhang, Ultra-low sintering temperature ceramics for LTCC applications: a review. J. Mater. Sci.: Mater. Electron. **26**, 9414–9423 (2015)
15. J.J. Bian, D.W. Kim, K.S. Hong, Microwave dielectric properties of $(Ca_{1-x}Zn_x)_2P_2O_7$. Mater. Lett. **59**, 257–260 (2005)
16. J.J. Bian, D.W. Kim, K.S. Hong, Microwave dielectric properties of $A_2P_2O_7$. Jpn. J. Appl. Phys. **43**, 3521–3525 (2004)
17. X.Q. Song, K. Du, Z.Y. Zou, Z.H. Chen, W.Z. Lu, S.H. Wang, W. Lei, Temperature-stable $BaAl_2Si_2O_8$-$Ba_5Si_8O_{21}$-based low-permittivity microwave dielectric ceramics for LTCC applications. Ceram. Int. **43**, 14453–14456 (2017)
18. Y.J. Chu, J.H. Jean, Low-fire processing of microwave $BaTi_4O_9$ dielectric with crystalline CuB_2O_4 and $BaCuB_2O_5$ additives. Ceram. Int. **39**, 5151–5158 (2013)
19. H. Zhu, M. Liu, H. Zhou, L. Li, A. Lv, Study on properties of CaO-B_2O_3-SiO_2 system glass-ceramic. Mater. Res. Bull. **42**, 1137–1144 (2007)
20. U. Došler, M.M. Kržmanc, D. Suvorov, Phase evolution and microwave dielectric properties of MgO-B_2O_3-SiO_2-basedglass-ceramics. Ceram. Int. **38**, 1019–1025 (2012)
21. Z.J. Qing, B. Li, Y.X. Li, H. Li, S.R. Zhang, Microstructure and properties of ZnO doped CaO-Al_2O_3-SiO_2 ceramic for LTCC applications. J. Mater. Sci.: Mater. Electron. **26**, 1512–1517 (2015)
22. D.H. Jiang, J.J. Chen, B.B. Lu, J. Xi, F. Shang, J.W. Xu, G.H. Chen, Preparation, crystallization kinetics and microwave dielectric properties of CaO-ZnO-B_2O_3-P_2O_5-TiO_2 glass-ceramics. Ceram. Int. **45**, 8233–8237 (2019)
23. H.Y. Zhu, R.L. Fu, S. Agathopoulos, J. Fang, G.J. Li, Q.J. He, Crystallization behaviour and properties of BaO-CaO-B_2O_3-SiO_2 glasses and glass-ceramics for LTCC applications. Ceram. Int. **44**, 10147–10153 (2018)
24. S. Zhang, H. Su, H. Zhang, Y. Jing, X. Tang, Microwave dielectric properties of $CaWO_4$-Li_2TiO_3 ceramics added with LBSCA glass for LTCC applications. Ceram. Int. **42**, 15242–15246 (2016)
25. P. Pascuta, G. Borodi, E. Culea, Influence of europium ions on structure and crystallization properties of bismuth borate glasses and glass ceramics. J. Non-Cryst. Solids **354**, 5475–5479 (2008)
26. T. Takada, S.F. Wang, S. Yoshikawa, S.J. Jang, R.E. Newnham, Effect of glass additions on BaO-TiO_2-WO_3 microwave ceramics. J. Am. Ceram. Soc. **77**, 1909–1916 (1994)
27. B.W. Hakki, P.D. Coleman, A dielectric resonator method of measuring inductive capacities in the millimeter range. IEEE Trans. Microw. Theory Tech. **8**, 402–410 (1960)
28. B.D. Silverman, Microwave absorption in cubic strontium titanate. Phys. Rev. **125**, 1921–1930 (1962)
29. D.H. Jiang, J.J. Chen, B.B. Lu, J. Xi, G.H. Chen, A new glass-ceramic with low permittivity for LTCC application. J. Mater. Sci.: Mater. Electron. **29**, 18426–18431 (2018)
30. C.C. Xia, G.H. Chen, C.L. Yuan, C.R. Zhou, Low-temperature co-fired $LiMnPO_4$-TiO_2 ceramics with near-zero temperature coefficient of resonant frequency. J. Mater. Sci.: Mater. Electron. **28**, 13970–13975 (2017)
31. M.S. Ma, Z.Q. Fu, Z.F. Liu, Y.X. Li, Fabrication and microwave dielectric properties of CuO-B_2O_3-Li_2O glass-ceramic with ultra-low sintering temperature. Ceram. Int. **43**, 292–295 (2017)
32. Y. Xiang, J. Han, Y.M. Lai, S.H. Li, S. Wu, Y. Xu, Y.M. Zeng, L.M. Zhou, Z.H. Huang, Glass structure, phase transformation and microwave dielectric properties of CaO-B_2O_3-SiO_2 glass-ceramics with addition of La_2O_3. J. Mater. Sci.: Mater. Electron. **28**, 9911–9918 (2017)